Polytechnic Journal. 2022. 12(2): 180-192
ISSN: 2313-5727
http://journals.epu.edu.iq/index.php/polytechnic

POLYTECHNIC JOURNAL

RESEARCH ARTICLE

Flexural Behavior of Two-layers Reinforced Concrete Beams

Halmat B. Najm [1], Mereen H. Fahmi Rasheed [2]

[1] *Department of Civil Engineering, Erbil Technical College, Erbil Polytechnic University, Erbil, Kurdistan Region, Iraq*

[2] *Department of Civil Engineering, Erbil Technical College, Erbil Polytechnic University, Erbil, Kurdistan Region - Iraq*

***Corresponding author:**
Halmat B. Najm,
Department of Civil Engineering, Erbil Technical College, Erbil Polytechnic University, Erbil, Kurdistan Region, Iraq.

E-mail:
halmat.najm@epu.edu.iq

Received: 20 aug-2022
Accepted: 04 oct2022
Published: 1 February 2023

DOI
10.25156/ptj.v12n1y2022.pp180-192

ABSTRACT

High-strength concrete is used to reduce the size of the beams in addition to enhancing the strength, this leads to overestimated cost in comparison with normal-strength concrete while using normal-strength concrete leads to the overestimated amount of concrete (layer size) of the beam section. For balancing the condition between the cost and size of beams, the benefit of both materials is used, by using beams in two layers, high-strength concrete in the compression zone (top layer), which is more beneficial for beam strength, and normal strength concrete in tension zone (bottom layer), which is no need using high strength concrete the in-tension zone. This study investigates the flexural and shear behavior of reinforced concrete beams consisting of two layers with different concrete strengths (grades), for beams with and without shear reinforcement (stirrups), considering the effect of shear-span ratio, layer thickness, layer compressive strength, and the overlap time casting of the two layers. The experimental program consists of a total of nineteen reinforced concrete beams of dimension (125 mm x 250 mm) with a total length of 1200 mm, the beams are reinforced with longitudinal reinforcement (4Ø12mm) and using (Ø8mm) bar as transverse reinforcement (stirrups). The experimental results show that the crack pattern of the two-layer reinforced concrete is closer to the crack of the control beam with one layer. Increasing the compressive strength of the concrete of the top layer, the ultimate failure load increased by (8.35%, 15.6%, and 18.85%), with respect to the (control beam) with the full depth of normal concrete. By increasing the high-strength layer thickness, the value of shear strength (Vc) and ultimate shear strength (Vu) increased linearly. The casting overlap time of up to (60 min) can be used for casting two-layered reinforced concrete beams, which is recommended, beyond this time the strength of the shear strength (Vc) and, ultimate shear strength (Vu) decreases. With increasing the shear span ratio (a/d) from (1 to 1.5 and 2) the ultimate load failure decreased by (33% and 50%). The shear strength capacity decreases with increasing stirrup spacing.

Key Words: Two-layer RC beams, HSC beams, NSC beams, Shear strength, Ultimate shear strength.

1. INTRODUCTION

Concrete is one of the construction materials, which is the most widely used because it has many advantages such as cost-benefit, stable material supply, and a high level of durability. The size of the concrete beam section and arrangement of the reinforcement is providing the required resistance for moments and shears developed in the element. High-strength concrete (HSC) provides a better solution for reducing the sizes and weights of the concrete structural element (Parghi P.Eng. C.Eng and Modhera, 2008). So, it can reduce the cost of high-strength concrete (HSC) elements by using lower-strength concrete in the tension zone and high-strength concrete in the compression zone called a two-layers reinforced concrete beam. The beams consist of two different types of concrete layers: normal-weight concrete (NWC) and lightweight aggregate concrete (LWAC). The results show that except for crack spacing, the behavior of both control and two-layer beams was the same. The cracks of the two-layer beams were closer to each other than the cracks of the control beams. With increasing lightweight aggregate layer

In tension zone, the ultimate load capacity of beams was reduced (Adnan et al., 2021). Beams are made of two layers of various types of concrete. In the top layer, normal density concrete (NC) was mixed with a layer of fiber-reinforced lightweight concrete (FRLWC), steel fiber reinforcement of lightweight concrete increased the ductility in tension, and normal shear reinforcement decreased. Furthermore, the bending failure of these composite beams is less ductile than the bending failure of a normal reinforced concrete beam. With more fibers, the shear capacity increases (Nes and Overli, 2015). Two-layer beams (TLB) using

steel fibered high-strength concrete (SFHSC) in the compression zone and normal strength concrete (NSC) in the tensile zone. TLB has been improved to be more effective, and it has been shown that using the optimum steel fiber weight ratio in HSC allows for high-performance bending elements with similar elastic-plastic behavior to regular NSC bending elements (Iskhakov et al., 2014). Slab consisting of two-layer reinforced concrete HSC in the compression zone and NSC the in-tension zone by effecting delay overlap time between two-layer concrete (15 minutes and 60 minutes), using the HSC at the compression zone with a 60-minute time overlap between casting the two layers indicates a significant improvement (Yehia, 2020). The casting time between two concrete (cold joints) 120 minutes and 240 minutes indicate that specimens with a cold joint connection in normal concrete, as well as concrete with a superplasticizer (high early compressive strength), have lower quality (flexural and compressive), although concrete with fiber has a higher strength than normal concrete without a cold joint connection (Zega et al., 2021). The flexural behavior of a two-layer high-strength reinforced concrete beam is compared with a single-layer high-strength reinforced concrete beam. The behavior of the braking force of both beams was similar as well as the deflections. Both beams appeared the first crack at the same loading (Butean and Heghes, 2020). The flexural behavior of layered beams with steel fiber reinforced concrete (SFRC) external layers and RC internal layers the deflection layered beam is (42%) higher than the control beam, control beam showed less cracking than the layered beam. The deflection monolithic reinforced concrete beam was (0.7%) larger than the monolithic SFRL beam (Martínez-Pérez et al., 2017). The flexural behavior of concrete beams hybrid reinforced by continuous basalt fiber reinforced polymer (BFRP) bars and discrete steel fibers increasing the steel fiber volume ratio reduced deflection and crack width. At the service stage, increasing the steel fiber volume ratio had a larger effect than at the final stage. The deflections and cracking response of the beam with a 2.0 % steel fiber volume ratio were like those of the beam with a 1.5 % steel fiber volume ratio (Li et al., 2022). The compressive, splitting, tensile, and flexural strengths of concrete decreased as the time between pouring two layers of concrete increased (Bekem Kara, 2021). Several recent studies focused on the flexural behavior of two-layer reinforced concrete consisting of normal strength NSC in tension zone and steel fiber high strength in compression zone SHSC or NSC with steel fiber lightweight concrete. While this current investigation concentrated on the flexural behavior of two-layer reinforced concrete consisting of normal strength concrete NSC in the tension zone and high strength concrete HSC in the compression zone.

2. EXPERIMENTAL PROGRAM

The experimental program consists of a total of nineteen rectangular simply supported beams under a four-point load with and without transverse reinforced (stirrups) in the study area and with different compressive strengths, The beam cross-section dimensions are (125*250*1200) mm shown in Figure (1), with maximum nominal aggregate sizes of (12.5) were used in the experimental work. The specimen beams were divided into six groups shown in Table (), the beams are reinforced with longitudinal reinforcement (4Ø12mm), with transverse reinforcement in the study area, and the reinforcement used for stirrups was (Ø8mm). In beams, B1 to B3, the beams were subjected to the effect of the ratio of compressive strength of

high strength to normal strength with stirrups, group (A). Beams B4 to B7 are subjected to the effect of overlap time, group (B). Beams B8 to B11 are subjected to the effect of layer thickness group (C). Group (D) consist of beams (B12, B13, and B2) to study the effect of shear span ratio (a/d). Beams B15 to B 17 are subjected to the effect of the concrete compressive strength ratio without stirrups group (E). The last beams, B18 and B19 are subjected to the effect of stirrups space group (F) figure (2) illustrated the casting and curing of the specimens.

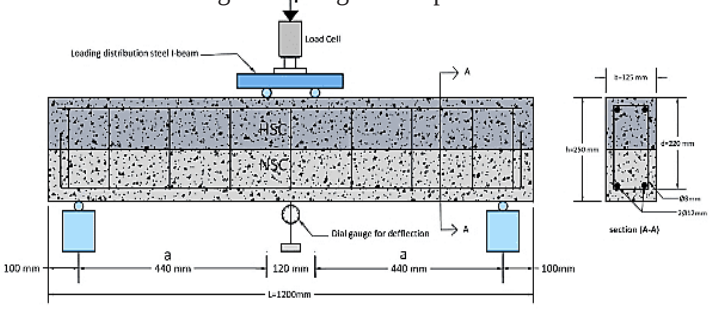

Figure (1) longitudinal and cross-section of the specimens

Figure (2) casting and curing of the specimens

fc': cylindrical compressive strength of concrete (MPa), HSC: high strength concrete, NSC: normal strength concrete, h_{HSC}: depth of the layer (top layer) mm, h_{NSC}: depth of the layer (bottom layer) mm

Groups	Beam No	fc`NSC (MPa)	fc`HSC (MPa)	fc`HSC / fc`NSC	h_{HSc} (mm)	h_{NSc} (mm)	$\frac{h_{HSc}}{h_{total}}$	Overlap time (min)	$\frac{a}{d}$	$\frac{L}{h}$	Note
				Effect of fc'_{HSc}/fc'_{NSc} with stirrups							
A	1	30	45	1.5	125	125	0.5	30	2	4	
	2	30	60	2	125	125	0.5	30	2	4	
	3	30	75	2.5	125	125	0.5	30	2	4	
				Effect of overlap time							
B	4	30	60	2	125	125	0.5	15	2	4	
	2	30	60	2	125	125	0.5	30	2	4	
	5	30	60	2	125	125	0.5	60	2	4	
	6	30	60	2	125	125	0.5	80	2	4	
	7	30	60	2	125	125	0.5	100	2	4	
				Effect of layer thickness							
C	8	30	-	-	-	250	-		2	4	Full NSC
	9	30	60	2	62.5	187.5	0.25	30	2	4	
	2	30	60	2	125	125	0.5	30	2	4	
	10	30	60	2	187.5	62.5	0.75	30	2	4	
	11	30	60	2	250	-	1	-	2	4	Full HSc
				Effect of ratio a/d							
D	12	30	60	2	125	125	0.5	30	1	4	
	13	30	60	2	125	125	0.5	30	1.5	4	
	2	30	60	2	125	125	0.5	30	2	4	
				Effect of $fc/_{HSC}/fc/_{NSC}$ without Stirrups							
E	14	30	-	-	-	250	-	-	2	4	Control beam
	15	30	45	1.5	125	125	0.5	30	2	4	
	16	30	60	2	125	125	0.5	30	2	4	Effect of $\frac{fc_{HSc}^{-}}{fc_{NSc}^{-}}$
	17	30	75	2.5	125	125	0.5	30	2	4	
				Effect of stirrups space							Ø8 mm stirrups spacing
F	16	30	60	2	125	125	0.5	30	2	4	0
	18	30	60	2	125	125	0.5	30	2	4	100
	2	30	60	2	125	125	0.5	30	2	4	150
	19	30	60	2	125	125	0.5	30	2	4	200

Table (1) experimental program of the specimens

3. MATERIAL PROPERTIES

3.1 Cement

Mass's Ordinary Portland Cement is used to design normal and high strength Concrete Mixes. The physical and chemical

properties of cement are tested and verified according to the specifications of (ASTM - C150).

3.2 Fine Aggregate (Sand)

Locally available sand from (The aski-Kalak source) was used. The sand is cleaned, and the maximum particle size was (4.75 mm), and the grading curve of the fine aggregate is shown in Figure (3). Also tested within the upper and lower limits of the (ASTM - C33) specification.

3.3 Coarse Aggregate

The coarse aggregate used in the current experimental program was rounded river coarse aggregate, the gravel was locally available, the specific gravity of coarse aggregate was (2.69), the bulk density of coarse aggregate was (1695 kg/m3), and the sieve analysis of the aggregate of maximum nominal size (12.5 mm) is shown in Figure (4), and the test result was within the lower and upper limit of the specification of (ASTM-C33).

3.4 water

The water used during the experimental program, both in producing concrete and in curing all beams specimens, was tap clean drinking fresh water free from impurities

3.5 Silica Fume

Silica Fume is a binder material that can be added directly to concrete or combined with cement. it is used to enhance concrete properties. The silica fume used in the present study is in the production of ECA MICRO SILICA-D which has the properties of increasing compressive and flexural strength, reducing permeability, and increasing durability. The physical and chemical properties of the silica fume are tested and checked according to the specification of (ASTM-C1240).

3.6 Superplasticizer

Superplasticizer is the most popular admixture to the concrete mix. It is available generally in a liquid. The superplasticizer used in the present study is in the production of Sika ® ViscoCrete ® -1316 Hi-Tech meets the requirements of (ASTM-C494). It is a high-range water-reducing, retarding, and slump retaining admixture. It is added to the mix with a ratio of about (0.1% to 2%) of cement weight.

4. MIXING AND MIX PROPORTION

According to the American Concrete Institute Code (ACI CODE-318-19) recommendations, many trial mixes were designed for concrete with nominal aggregate size (12.5mm) to obtain the various concrete compressive strength. thirteen trial mixes were done to get different classes of strengths. The amounts of materials required for (1 m3) of concrete in each mix are listed in Table (2).

Table (2) Selected concrete mixes per one meter cube of concrete

Trail No.	fc' (MPa)	C	SF	S	G	SP	Water
		Kg					Litter/m^3
4	30	325	-	812	975	-	172
7	45	550	-	655	940	0.55	198
10	60	600	-	600	990	2.52	192
13	75	650	65	572	1072	13	178

C: Cement, SF: Silica Fume, S: Sand, G: Gravel and SP: Super Plasticizer.

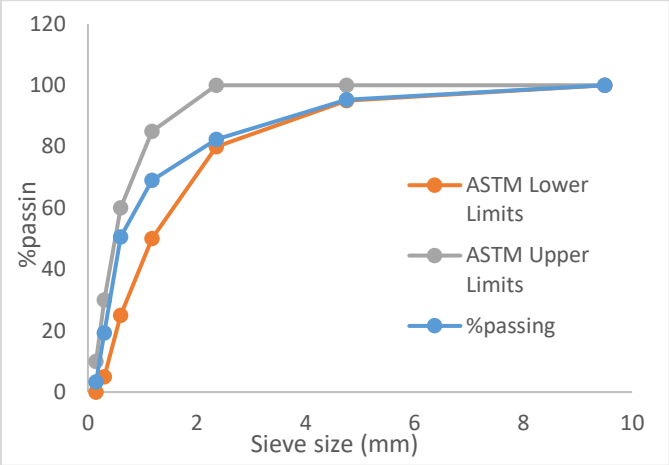

Figure (3) Grading curve for the fine aggregate with ASTM limits

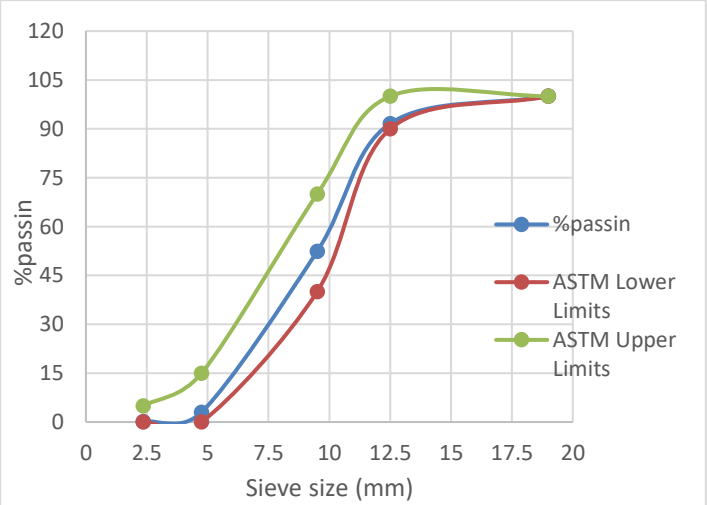

Figure (4) Grading curve for coarse aggregate with ASTM limits

5. RESULTS AND BEHAVIOR OF TESTED BEAMS

The beams were subjected to two equal point (four-point load test). The primary hypothesis of this study is on the flexural and shear behavior of reinforced concrete beams consisting of two layers with different concrete strengths (grades). First flexural

cracking shear (Vc1), diagonal shear force (Vc), ultimate shear strength (Vu), the experimental results of nineteen reinforced concrete beams, and the results of testing all control specimens for compressive strength and splitting tensile strength of concrete also shown in Table (3).

a/d: shear span ratio, fsp: Splitting tensile strength (MPa), Pc: Cracking load (kN), Pu: Ultimate failure load (kN), Vc1: Flexural first cracking shear (kN), Vc: shear strength of the beam (kN), Vu: Ultimate shear strength (kN).

6. CRACK PATTERN AND FAILURE MODE

6.1 Crack pattern and failure mode of the group (A)

Several crack patterns and failure modes were observed in the

Table (3) experimental result of all specimens

Groups	Beam No.	$\frac{h_{HSC}}{h_{total}}$	Overlap time (min)	$\frac{a}{d}$	$\frac{L}{h}$	fc`$_{NSC}$ (MPa)	fc`$_{HSC}$ (MPa)	$\frac{fc`HSC}{fc`NSC}$	$f_{sp\ (NSC)}$ (MPa)	f_{sp} (HSC) (MPa)	$P_{c\ (kN)}$	$P_{u\ (KN)}$	Vc1 (kN)	V_c (kN)	V_u (kN)	Remark
							Effect of (fc`$_{HSC}$)/(fc`$_{NSC}$) with stirrups									
	1	0.5	30	2	4	34.54	47.3	1.37	3.2	3.51	63.6	136.2	17.8	31.8	68.1	
A	2	0.5	30	2	4	33.5	63.38	1.89	3.37	3.91	72.6	145.3	17.4	36.3	72.65	
	3	0.5	30	2	4	33.14	74.65	2.25	3.54	4.61	75.6	149.4	18.05	37.8	74.7	
							Effect of overlap time									
	4	0.5	15	2	4	33.87	60.73	1.8	3.26	3.97	74.3	145.8	21.5	37.15	72.9	
	2	0.5	30	2	4	33.5	63.38	1.89	3.37	3.91	72.6	145.3	17.4	36.3	72.65	
B	5	0.5	60	2	4	34.73	59.48	1.72	3.26	3.81	73.4	143.8	18.7	36.7	71.9	
	6	0.5	80	2	4	35.52	62.75	1.77	3.3	3.99	70.5	143	18.55	35.25	71.5	
	7	0.5	100	2	4	34.72	62.47	1.8	3.24	3.89	83.2	142.8	19.7	41.6	71.4	
							Effect of layer thickness									
	8		30	2	4	33.87	-	1.8	3.26	3.97	55.7	125.7	25.2	27.85	62.85	Full NSC control beam
	9	0.25	30	2	4	34.16	61.75	1.8	3.24	3.59	69.5	127.2	19.3	34.75	63.6	
C	2	0.5	30	2	4	33.5	63.38	1.89	3.37	3.91	72.6	146.7	17.4	36.3	72.65	
	10	0.75	30	2	4	34.16	61.75	1.8	3.24	3.59	72.3	139	17.35	36.15	69.5	
	11	1	30	2	4	-	62.47	1.8	3.24	3.89	82.4	150.4	18.95	41.2	75.2	Full HSC control beam
							Effect of shear span ratio a/d									
	12	0.5	30	1	4	34.68	60.49	1.75	3.14	3.87	138	289.9	44.7	69	144.95	
D	13	0.5	30	1.5	4	34.68	60.49	1.75	3.14	3.87	117.5	194.6	51.8	58.75	97.3	
	2	0.5	30	2	4	33.5	63.38	1.89	3.37	3.91	72.6	145.3	17.4	36.3	72.65	
							Effect of (fc`$_{HSC}$)/(fc`$_{NSC}$) without stirrups									
	14		30	2	4	35.52	62.75	1.77	3.3	3.99	56.7	111.5	16.15	28.35	55.75	Full NSC control beam
E	15	0.5	30	2	4	34.54	47.3	1.37	3.2	3.51	65.4	114	24.8	32.7	57	
	16	0.5	30	2	4	33.5	63.38	1.89	3.37	3.91	67.5	115.3	19.6	33.75	57.65	
	17	0.5	30	2	4	33.14	74.65	2.25	3.54	4.61	72.4	118.6	20.2	36.2	59.3	
							Effect of stirrups spacing									Ø8 mm stirrups spacing
	16	0.5	30	2	4	33.5	63.38	1.89	3.37	3.91	67.5	115.3	19.6	33.75	57.65	0
	18	0.5	30	2	4	34.14	62.54	1.84	3.29	3.66	79.6	148.5	17.55	39.8	74.25	100
F	2	0.5	30	2	4	33.5	63.38	1.89	3.37	3.91	72.6	145.3	17.4	36.3	72.65	150
	19	0.5	30	2	4	34.14	62.54	1.84	3.29	3.66	71.2	137.4	19.7	35.6	68.7	200

experiments. For beams of the group (A) was subjected different compressive strength layers. The first flexural crack appeared at the center of the beams at load level between (17.4 to 25.7 kN) for the specimens, it was followed by the first diagonal shear crack level between (27.85 to 37.8 kN). As the loading was increased, additional diagonal shear and flexural cracks developed, spreading throughout the span. From the internal edge of the supports to the center of the load-bearing plate, the diagonal shear cracks had developed gradually. The flexural cracks also spread toward the top of the beam, and a few additional small diagonal cracks were seen. With increasing the layer of the compressive strength, the ultimate failure load increased (8.35%, 15.6%, 18.85%) of beams (B1, B2, and B3) with respect to B8 (control) beam with the full depth normal concrete. All beams in this group failed in flexural at the load level (125.7, 136.2, 145.3, 149.4 kN). The final crack pattern of the beams was shown in Figure (5).

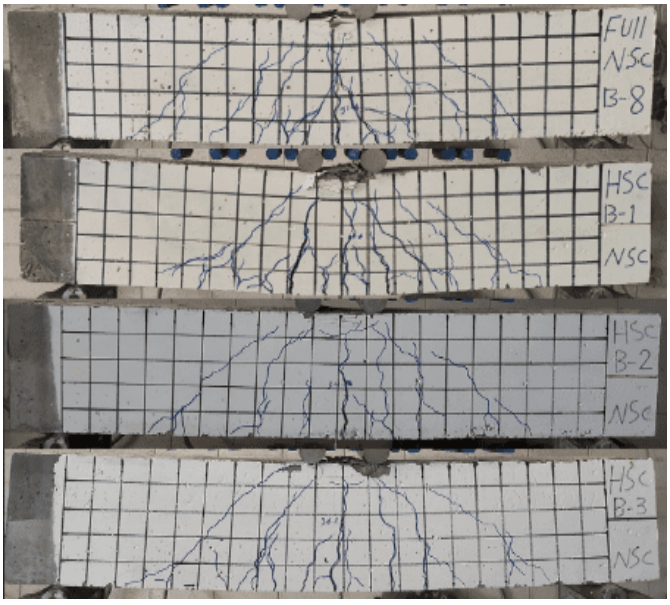

Figure (5) Group (A) Cracking pattern of the test specimens (B1, B2, B3, and B8)

6.2 Crack pattern and failure mode of the group (B)

The specimens of this group were affected by the overlap time of layer casting. During the tested of the specimens, several crack patterns and failure modes were observed. The first flexural crack appeared at the mid-span at a load level of between (17.4 to 25.7 kN), while the first diagonal shear crack appeared close to the left support at a load level of between (27.85 to 41.6 kN). When the loading was increased, additional diagonal shear and flexural cracks developed, spreading throughout the span. From the internal edge of the supports to the center of the load-bearing plate, the diagonal shear cracks had developed gradually. The flexural cracks also spread toward the top of the beam, and a few additional small diagonal cracks were seen. The flexural cracks grew corresponding to the yielding of steel bars with the increase of loads. Up to (30 min) ultimate load greater than the (60 to 100 min). all specimens in this group failed in flexural at the level of load (125.7, 145.8, 145.3, 143.8, 143, 142.8 kN) for beams (B8, B4, B2, B5, B6, and B7) respectively. The ultimate load increased by (16%, 15.6%, 14.4%, 13.8%, and 13.6%) for beams (B4, B2, B5, B6, and B7) with respect to the control beam with full depth normal concrete (B8). The final crack of the specimens was given in Figure (6).

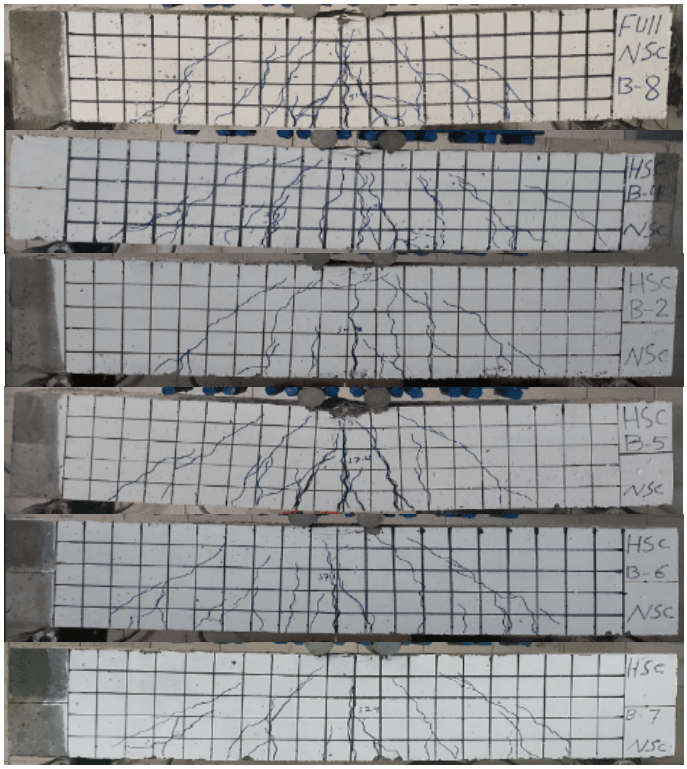

Figure (6) Group (B) Cracking pattern of the test specimens (B2, B4, B5, B6, B7, and B8)

6.3 Crack pattern and failure mode of the group (C)

This group was subjected to different layer thickness of NSC and HSC. Several crack patterns and failure modes were observed in the experiments. It was observed that the first flexural crack appeared at the center of the specimens. Specimen (B2) consists of (50%) of HSC had an earlier appearance of flexural crack at (17.4 kN), and in other specimens (B8, B9, B2, B10, B11) the flexural crack seen at the level load of (25.2, 19.3, 17,4, 17.35, 18.95 kN) respectively, the diagonal shear crack occurred at (27.85, 34.75, 36.3, 36.35, 36.15, 41.2 kN) respectively. When the loading was increased, additional diagonal shear and flexural cracks developed, spreading throughout the span. From the internal edge of the supports to the center of the load-bearing plate, the diagonal

shear cracks had developed gradually. The flexural cracks also spread toward the top of the beam, and a few additional small diagonal cracks were seen. With increasing loads, the flexural cracks increased in proportion to the yielding of steel bars. The ultimate load for specimens was (125.7, 127.2, 145.3, 139, and 150.4 kN) for (B8, B9, B2, B10, B11) respectively. The ultimate load increased by (1.6%, 15.6%, 10.6%, and 19.65%) with respect to the control beam (B8). All beams in this group failed in flexural. The final crack pattern as shown in Figure (7)

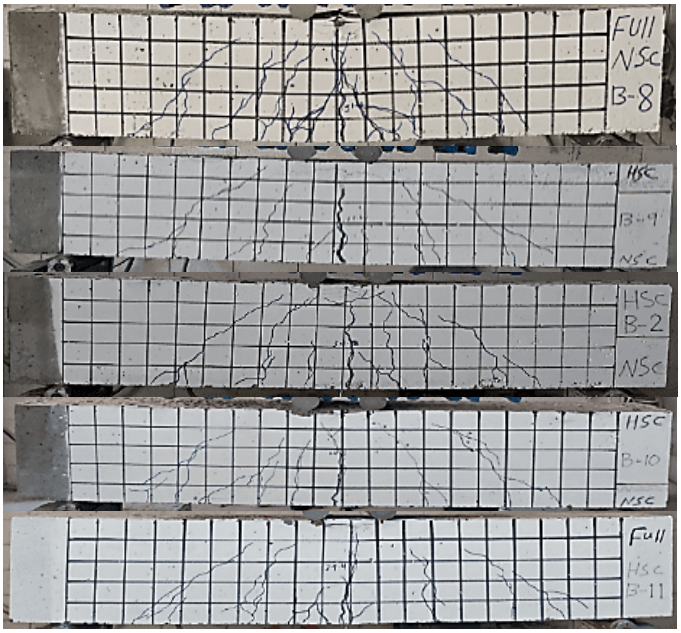

Figure (7) Group (C) Cracking pattern of the test specimens (B2, B8, B9, B10, and B11)

6.4 Crack pattern and failure mode of the group (D)

In this group the difference in the shear span ratio were studied span ratio (a/d), several cracks, and modes of failure was recorded for all specimens. The first flexural crack appeared at the mid-span at load levels of (44.7, 51.8, and 17.4 kN) followed by the first diagonal shear crack at a load level of (69, 58.75, and 36.4 kN) for (B12, B13, and B2) respectively. With the increase of loading, more diagonal shear and flexural cracks were propagated over the whole span of the beams, also It was found that the cracks developed an angle of (40°-50°) near the ends of both specimens (B12, and B13) These cracks dispersed throughout both sides of the beam. The flexural cracks grew corresponding to the yielding of steel bars with the increase of loads. With decreasing the shear span ratio (a/d) from (2 to 1.5 and 1) the ultimate load failure increased by (99% and 34%) for beams (B12, and B13) with respect to (B2) All specimens failed in flexural at load (289.9, 194.5, 145.3) respectively. The final crack pattern was given in Figure (8).

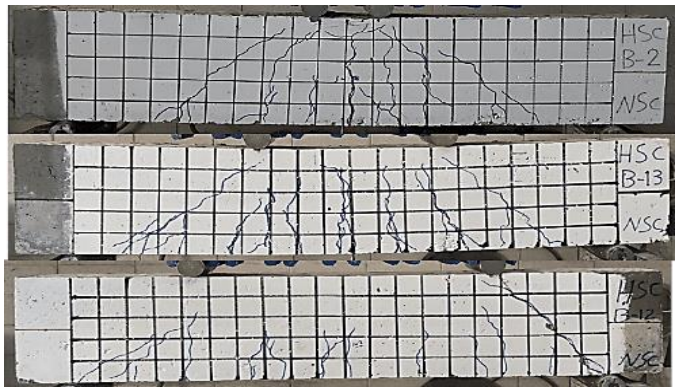

Figure (8) Group (D) Cracking pattern of the test specimens (B12, B13, and B2)

6.5 Crack pattern and failure mode of the group (E)

This group is like group (A) different compressive strength layers was used while no stirrups were used for the beams. This group had more diagonal shear cracks. The flexural cracks also spread but don't toward the top of the beam for all specimens in this group as shown in Figure (9). The first flexural crack was seen at load (16.15, 24.8, 19.6, and 20.2 kN). Also, the first diagonal shear appeared at load (28.35, 32.7, 33.75, and 36.2) for specimens (B14, B15, B16, and B17) respectively. With increasing the applied load, the diagonal shear crack begins at the interior face of the support and propagate approximately (45) degree toward the neutral axis of the beam. By increasing the layer of HSC ratio, the ultimate load was raised by (2.24%, 3.4%, and 6.37%) for beams (B15, B16, and B17) with respect to beam (B14) consist full depth normal concrete without stirrups respectively. the ultimate load failure of the specimens was (111.5, 114, 115.3, and 118.6 KN).

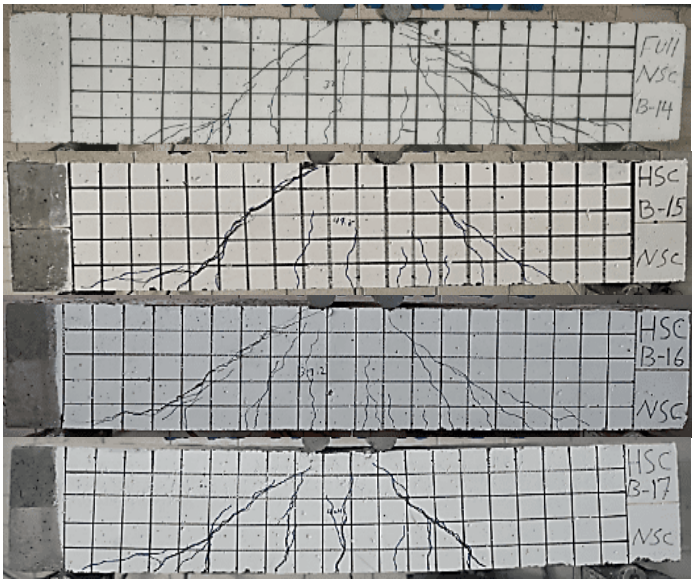

Figure (9) Group (E) Cracking pattern of the test specimens

(B14, B15, B16, and B17)

6.6 Crack pattern and failure mode of the group (F)

In this group the effect of spacing between stirrups was studied. the first flexural crack was noticed at the mid-span at a load level of (19.6, 17.55, 17.7, and 19.7 kN) and complied with the first diagonal shear crack at a load level of (33.75, 39.8, 36.3, and 35.6 kN) also, the failure load is recorded at a load level of (115.3, 148.4, 145.3 137 kN) for beams (B16, B18, B2, and B19). The mode of failure depended on the stirrup spacing, with decreasing the space between stirrups of the two-layer reinforced concrete the ultimate failure load was increased by (28.7, 26, and 19.17%), for beams (B18, B2, and B19) with respect to (B16) without stirrups respectively. as shown in Figure (10).

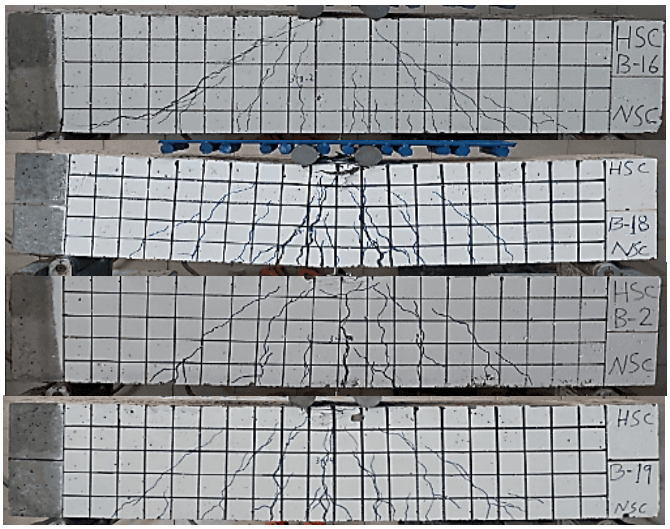

Figure (10) Group (F) Cracking pattern of the test specimens (B2, B16, B18, and B19)

7. MEASURED LOAD-DEFLECTION CURVES

For all specimens Experimentally obtained deflections at the mid-span of the beams. When the load increased gradually, the mid-span deflection of each beam showed a similar crack pattern. The deformation of deflection of all the specimens shows with the previous figures of the crack pattern.

In group (A) effected by the layered concrete compressive strength ratio, Figure (11) shows the measured load-deflection curves for beams (B1, B2, B3, and B8). The elastic region is represented by the linear rising limb which has a greater angle until it reaches the linear limit value of (130, 140, 120, and 125.7 kN) with a corresponding deflection of (3.08, 3.38, 2.97, and 3.32 mm) respectively but (B2, and B8) has too little plastic region range. By increasing the layer compressive strength, the ultimate load was increased, and the maximum applied load over the plastic region was (136.2, 145.3, 149.94, and 125.7 kN) with a maximum deflection at the mid-span of specimens (4.01, 3.64, 6.66, and 3.32 mm) respectively. The reason of this change due to increasing the compressive strength of top layer.

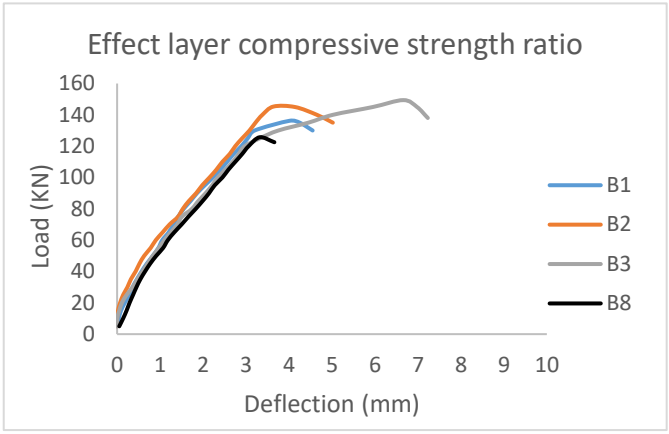

Figure (11) Deflection at mid-span group (A)

In group (B) affected by the overlap time of the casting of two layers of specimens. The elastic region is represented by the linear rising limb which has a greater angle until it reaches the linear limit value of (125.7, 125, 140, 140, 125, and 135 kN) with a corresponding deflection of (3.32, 2.79, 3.38, 2.89, 3.44, and 3.88mm) for specimens (B8, B4, B2, B5, B6, and B7) respectively. The maximum applied load over the plastic region was (125.7, 145.8, 145.3, 143, and 142.8 kN) with a maximum deflection at the mid-span of specimens (3.32, 4.68, 3.15, 7.54, and 4.93 mm). it was given in Figure (12).

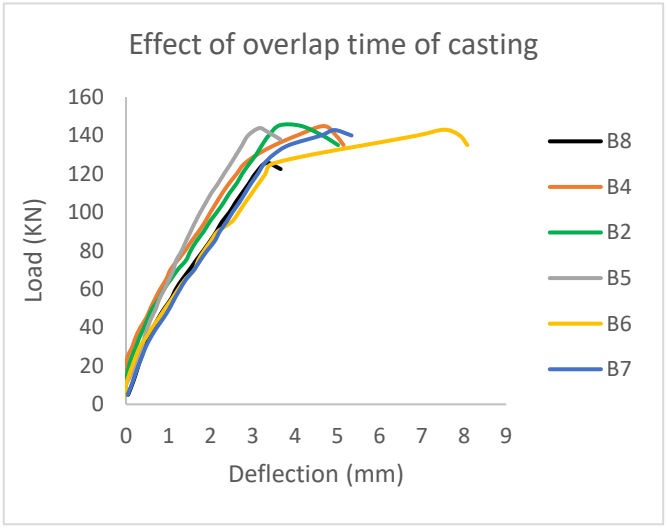

Figure (12) Deflection at mid-span group (B)

Group (C) was affected by the concrete layer thickness, the measured deflection was increased linearly until the applied load reached (125.7, 120, 140, 115, and 135 kN) with a corresponding deflection of (3.32, 3.44, 3.38, 3.15, and 3.69 mm) for specimens of (B8, B9, B2, B10, and B11) respectively. The maximum applied load over the plastic region was (125.7, 127.2, 145.3,139,

and 150.4 kN) with the deflection at the mid-span of specimens (3.32, 4.03, 3.64, 7.39, and 8.04 mm). illustrated in Figure (13). The reason of improvement the behavior, the increasing of the top layer thickness which is the high strength concrete.

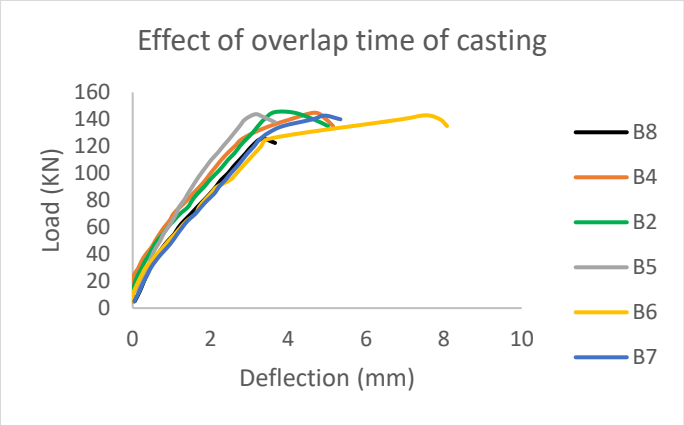

Figure (13) Deflection at mid-span group (C)

For group (D) effected by shear span ratio (a/d). The elastic region is represented by the linear rising limb which has a greater angle until it reaches a peak value of (280, 190, and 140 kN) with a corresponding deflection of (3.72, 3.69, and 3.38 mm) for specimens of (B12, B13, and B2) respectively. By decreasing the ratio of (a/d) from (2 to 1.5, and 1) the measured deflection at mid-span was increased by (5, and 12%) for specimens (B13 and, B12). The maximum applied load over the plastic region was (289.9, 194.5, and 145.3 kN) with a maximum deflection at the mid-span of the specimens (4.1, 3.84, and 3.64 mm). as shown in Figure (14). When (a/d) was increased, the behavior of the beam reach to the slender beam which is showed lower shear strength than beams with smaller (a/d).

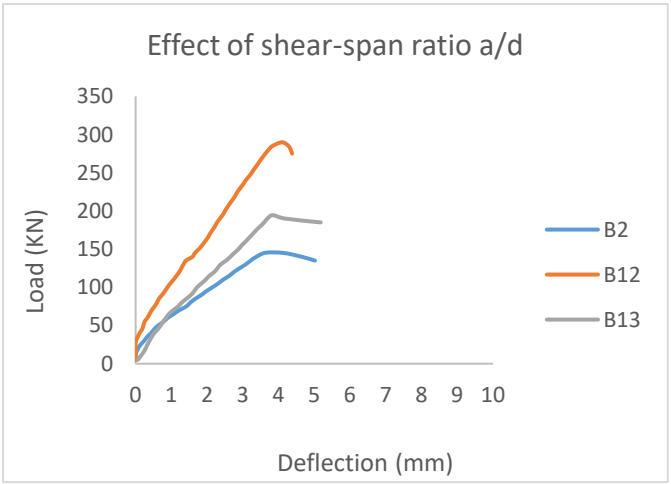

Figure (14) Deflection at mid-span group (D)

Group (E) effected by layer compressive strength without stirrups, the deflection of the control beam with full normal strength greater than other beams consisting of two layers. The elastic region is represented by the linear rising limb which has a greater angle until it reaches a peak value of (110, 115, 115,3, and 118.6 kN) with a corresponding maximum deflection at mid-span (3.71, 3.12, 3.82, and 3.32 mm). for specimens of (B14, B15, B16, and B17). The ultimate load was (111.5, 115, 115.3, and 118.6 kN). The applied load was discontinuous at the plastic region because the beams were without stirrups. It is given in figure (15). The reason of this change due to increasing the compressive strength of top layer.

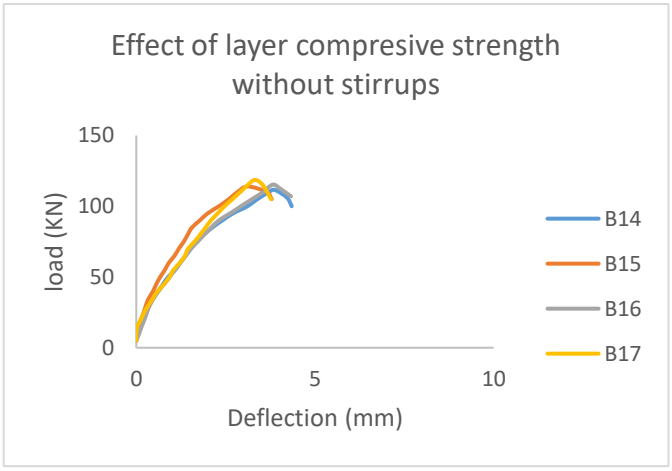

Figure (15) Deflection at mid-span group (E)

Group (F) effected by stirrup spacing. The elastic region is represented by the linear rising limb which has a greater angle until it reaches a peak value of (115,3, 135, 140, and 125 kN) with a corresponding deflection of (3.82, 3.52, 3.38, and 3.58 mm) for specimens of (B16, B18, B2, and B19) respectively. The maximum applied load over the plastic region was (148.4, 145.3, and 137.2 kN) with a maximum deflection at the mid-span of the specimens (4.43, 3.64, and 5.15mm) for beams (B18, B2, and B19) respectively, because of the participation of the transverse reinforcement (stirrups). Illustrated in Figure (16).

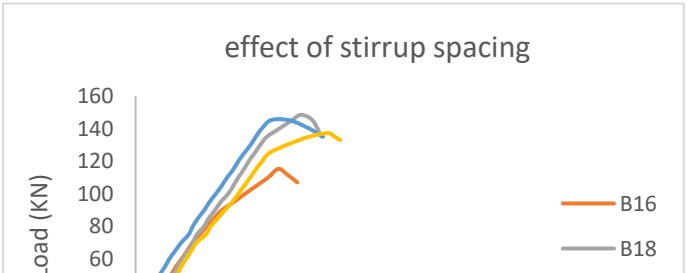

Figure (16) deflection at mid-span group (F)

8. Effect of the layer's compressive strengths on the shear capacity of the beams.

Figure (17) effect of concrete compressive ratio on (Vc &Vu)

Group	Beam No.	Overlap time (min)	Vc (kN)	% Increase	Vu (kN)	% Increase
B	8	0	27.85	-	62.85	-
	4	15	37.15	33.4	72.9	016
	2	30	36.3	30.3	72.65	0.16
	5	60	36.7	31.8	71.9	14.4
	6	80	35.25	26.6	71.5	13.8
	7	100	41.6	49.4	71.4	13.6

The cracking shear force (Vc) and ultimate shear strength (Vu) of the two-layer beams increased linearly with an increasing compressive strength ratio between the two layers (37%, 89%, 125%), the value of shear strength (Vc) increased by (14.2%, 30.3%, and 35.7%) respectively also the value of ultimate shear strength (Vu) increased by (8.4%, 15.6%, and 18.9%) respectively concerning the control beam (B8) as shown in Figures (17). The effect of the layer compressive strength ratio ($fc`_{HSC}$)/($fc`_{NSC}$) on (Vc) is greater than (Vu) by (50 to 70%). So, the compressive strength of concrete layers has a direct effect on the shear strength of concrete. Table (4) shows the experimental value of shear strength (Vc) and ultimate shear strength (Vu) of the specimens with different compressive strength ratios.

Table (4) experimental data of (Vc & Vu) group (A)

Group	Beam No.	$fc`_{NSC}$	$fc`_{HSC}$	($fc`_{HSC}$)/($fc`_{NSC}$)	Vc (KN)	% Increase	Vu (KN)	% Increase
A	8	33.87	33.87	1	27.85	-	62.85	-
	1	34.54	47.3	1.37	31.8	14.2	68.1	8.4
	2	33.5	63.38	1.89	36.3	30.3	72.65	15.6
	3	33.14	74.65	2.25	37.8	35.7	74.2	18.9

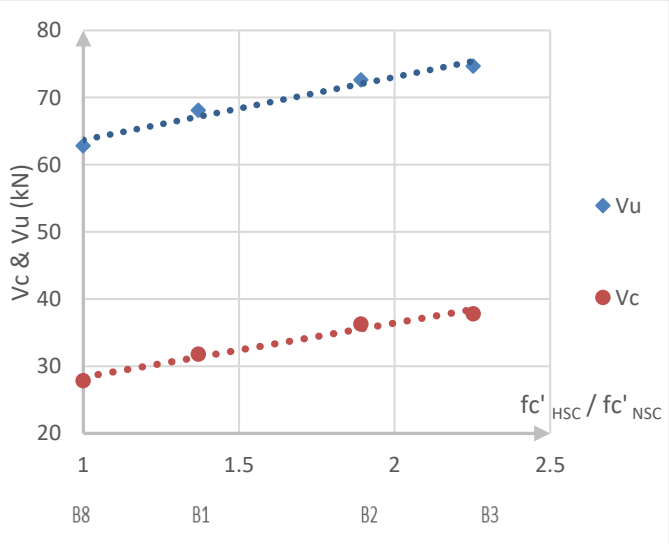

9. Effect of the overlap time casting on the shear capacity of the beams

Table (5) present the experimental value of shear strength (Vc) and ultimate shear strength of the specimens at a different time of casting two-layer of concrete.

Table (5) experimental data of (Vc & Vu) group (B)

According to Table (5) when the overlap time is zero the value of shear strength (Vc) and ultimate shear strength (Vu) control beam is lower than other beams consisting of two-layer reinforced concrete beams with different overlap times. Up to 60 min overlap time concrete shear strength (Vc) increases between (30 to 33 %) then the concrete shear strength decreases to (26.6 %). Likewise, ultimate shear strength (Vu) rises by (14 to 16%) up to 60 min then the strength decreased by (13.6%) at an overlap time of 100 min, as shown in Figures (18). It can be concluded that the casting overlap time of up to (60 min) can be used for casting two-layered reinforced concrete beams, which is recommended, beyond this time the strength of the beam (Vc &Vu) decreases.

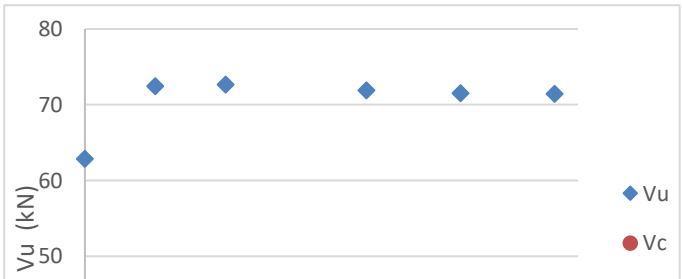

greater than (Vu).

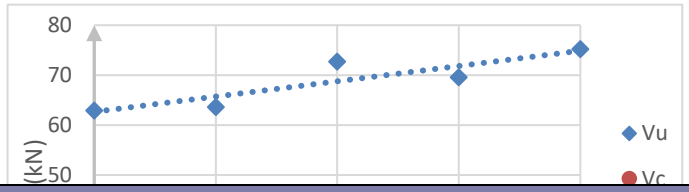

Group	Beam No.	h_{HSC} (mm)	h_{total} (mm)	$\frac{h_{HSC}}{h_{total}}$	Vc (kN)	% Increase	Vu (kN)	% Increase
	8	0	250	0	27.85	-	62.85	-
	9	62.5	250	0.25	34.75	24.8	63.6	1.2
C	2	125	250	0.5	36.3	30.3	72.65	15.6
	10	187.5	250	0.75	36.15	29.8	69.5	10.6
	11	250	250	1	41.2	41.2	75.2	19.65

Figure (18) Value of (Vc & Vu) with different overlap time

Figure (19) Effect of the different HSC layer ratios on (Vc & Vu)

10. Effect of concrete layer thickness on the shear capacity of the beams

Table (6) shows the experimental results of shear strength (Vc) and ultimate shear strength (Vu) of the beams with a different layer thickness of concrete.

Table (6) experimental data of (Vc & Vu) group (C)

The shear strength and ultimate shear strength of the control beam are lower than the beams consisting of two-layer with a different layer thickness of high-strength concrete. for the beam consisting of (0.25h) of high strength layer ratio, the concrete shear strength increased by (24.2%), and ultimate shear strength (Vu) increased by (1.2%). When the high strength layer rises to (0.5h), (Vc) and (Vu) increase by (30.3 and 15.6%) respectively. For the high strength layer of (0.75h), (Vc) increased by (29.8%) and (Vu) by (10.6%). When the high strength layer ratio reaches (1), means the beam consisting of full high strength concrete (Vc) increased by (48%), and (Vu) by (19.65%). This means that by increasing the high strength layer ratio, the value of (Vc and Vu) increased linearly as demonstrated in Figures (19). Also, the effect of the high strength concrete layer thickness on (Vc) is

11. Effect of shear span ratio (a/d) on the shear capacity of the beams

Table (7) shows the experimental results of shear strength (Vc) and ultimate shear strength (Vu) of the beams with different shear span ratios a/d.

Table (7) experimental data of (Vc & Vu) group (D)

Group	Beam No.	a (mm)	d (mm)	$\frac{a}{d}$	Vc (kN)	% Reduce	Vu (kN)	% Reduce
	12	220	220	1	69	-	144.95	-
D	13	330	220	1.5	58.75	%15	97.3	33%
	2	440	220	2	36.2	47.4	72.65	50%

Table (7) presented the value of (Vc & Vu) by affecting the shear span ratio (a/d). With the increase in the shear span ratio (a/d), the shear capacity of the two-layer concrete beams decreases

gradually. Figures (20) show the influence of the shear span–ratio (a/d) on the shear capacity. With a smaller shear span ratio, the amount of (Vc & Vu) is increased, for (a/d = 1.5) (Vc) decreased by (15%), and (Vu) by (33%). For (a/d = 2) (Vc) decreased by (47.4%) and (Vu) decreased by (50%). The effect of (a/d) on the ultimate shear strength (Vu) is greater than (Vc).

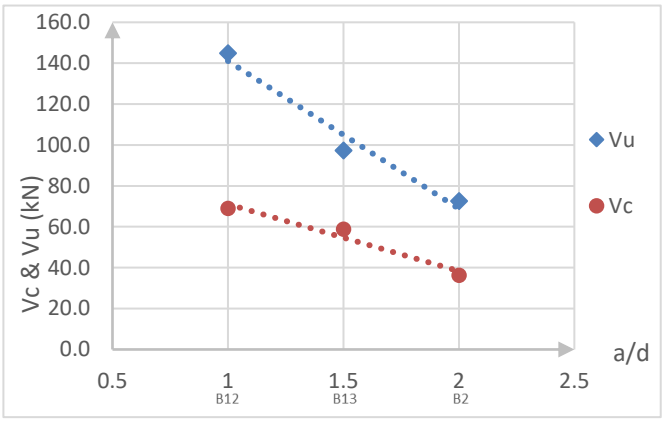

Figure (20) Effect of shear span ratio (a/d) on (Vc & Vu)

12. Effect of the layer compressive strength on the shear capacity of the beams without stirrups.

Table (8) shows the experimental value of shear strength (Vc) and ultimate shear strength of the specimens with different compressive strength ratios of the beams without stirrups.

Table (8) experimental data of (Vc & Vu) group(E)

Group	Beam No.	fc`NSC	fc`HSC	(fc`HSC)/(fc`NSC)	Vc (kN)	% Increase	Vu (kN)	% Increase
E	14	35.52	35.52	1	28.35	-	55.75	-
	15	34.54	47.3	1.37	32.7	15.3	57	2.24
	16	33.5	63.38	1.89	33.75	19	57.65	3.4
	17	33.14	74.65	2.25	36.2	27.7	59.3	6.4

The above table presented the experimental value of (Vc & Vu) two-layer reinforced concrete beams without stirrups. The capacity of shear strength and ultimate shear strength of the control beam is less than the other beam consisting of two-layer beams. The beams have a concrete compressive strength ratio (1.37) the amount of (Vc and Vu) is increased by (15.3 and 2.24%) respectively. When the compressive strength ratio is (1.89) the value of (Vc & Vu) rises to (19 and 3.4%). For the last beam which is the compressive strength ratio is (2.25) Again, the amount of (Vc) is going up to (27.7%) and (Vu) to (6.4%). With increasing the layer of high compressive strength ratio, the value of (Vc and Vu) is increased as shown in Figures (21). the effect of (fc`HSC /fc`NSC) on (Vc) is much greater than the (Vu). The behavior of the beams is the same as the beams with stirrup

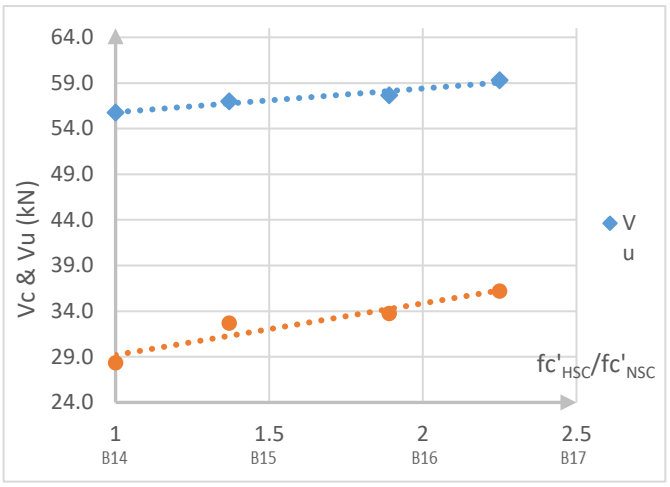

Figure (21) Effect of (fc`HSC)/(fc`NSC) without stirrups on (Vc & Vu)

13. Effect of stirrup spacing (amount of transverse) on the shear capacity of the beams

Table (9) present the experimental value of shear strength (Vc) and ultimate shear strength of the specimens with different amount of transverse reinforcement (spacing of stirrups).

Table (9) experimental data of (Vc & Vu) group (F)

Group	Beam No.	S (mm)	Vc (kN)	% Increase	Vu (kN)	% Increase
F	16	0	33.75	-	57.65	-
	18	100	39.8	18	74.75	29.7
	2	150	36.3	7.56	72.65	26
	19	200	35.6	5.5	68.7	19.2

Table (9) demonstrates the influence of different stirrup spacing on the result of cracking shear and ultimate shear force (Vc &

Vu) in the group (F). stirrup spacing has played a significant role in the capacity of shear strength. When the stirrup spacing is (200 mm) the amount of (Vc) increased by (15.5%) and (Vu) by (19.2%). For beams with stirrup, spacing is (150 mm) the value of (Vc &Vu) again rises to (7.56 and 26%) respectively. When reducing the space of stirrups to (100 mm) the amount of (Vc) is going up to (18 %) and (Vu) to (28.8%). With decreasing the spacing of stirrups, the capacity of shear strength is increased illustrated in Figures (22). Also, the effect of stirrup spacing on (Vu) is much greater than on (Vc).

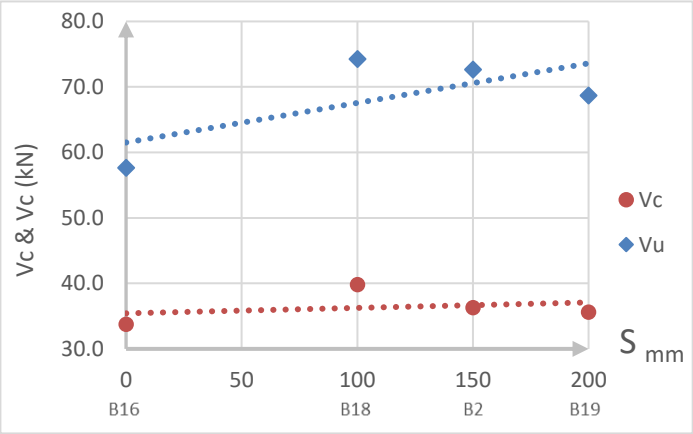

Figure (22) Effect of stirrup spacing on (Vc & Vu)

14. CONCLUSION

The following conclusions can be drawn from the experimental results obtained when testing the beams:-

1. The mid-span deflection and the crack pattern of the two-layer reinforced concrete beams are similar and closer to the crack pattern and behavior of the control beam (one layer of normal strength concrete)

2. With increasing the compressive strength of the top layer, the ultimate failure load increased by (8.35%, 15.6%, and 18.85%), concerning the (control beam) with the full depth of normal concrete.

3. The overlap time casting the two-layer up to (60 min) the cracking and ultimate shear strength are increased in general, then the values are decreased when the overlap time is increased to (100 min), this means that the two-layers can be cast in the first (60 min) after adding the other to the concrete mix, after this time the strength is decreased in general, and the concrete reaches to it is first setting time. So, the overlap time of layer casting is less than (60 min) is recommended.

4. By increasing the layer of high strength top thickness, the ultimate load increased by (1.2%, 15.6%, 10.6%, and 19.65%) concerning the control beam, corresponding to the layer thickness ratio (0.25, o.5, 0.75, and 1) respectively.

5. With the increase of the shear span ratio (a/d) from (1 to 1.5 and 2) the ultimate load failure decreased by (33% and 50%)

6. The effect of the layer compressive strength ratio (fc`HSC)/(fc`NSC) on shear strength (Vc) is greater than ultimate shear strength (Vu) by (50 to 70%).

7. The casting overlap time of up to (60 min) can be used for casting two-layered reinforced concrete beams, which is recommended, beyond this time the strength of the beam shear strength (Vc) and, ultimate shear strength (Vu) are decreases.

8. By increasing the high strength layer ratio, the value of shear strength (Vc) and ultimate shear strength (Vu) increased linearly

9. By increasing stirrup spacing the capacity of shear strength is decreasing.

REFERENCES

ACI CODE-318-(2019): Building Code Requirements for Structural Concrete and Commentary.

Adnan, O., Adai Al-Farttoosi, H., Al Bremani, H., (2021). Flexural behavior of two-layer beams made with normal and lightweight concrete layers. Period. Eng. Nat. Sci. PEN 9, 1124–1140.

ASTM C33 - Designation: C33/C33M− (2018) Standard Specification for Concrete Aggregates.

ASTM C150-(2020) - Standard Specification for Portland Cement. ASTM International, United States.

ASTM-C494-(2019). Classification of admixtures. American Society for Testing and Material.

ASTM-C1240-(2007). silica-fume-in-cementitious-mixture. American Society for Testing and Material.

Bekem Kara, İ., (2021). Experimental Investigation of the Effect of Cold Joint on Strength and

Durability of Concrete. Arab. J. Sci. Eng. 46, 10397–10408.

BS 1881 116 (1983) Testing Concrete. Method for Determination of Compressive Strength of Concrete Cubes.

Butean, C., Heghes, B., 2020. Flexure Behavior of a Two Layer Reinforced Concrete Beam. Procedia Manuf., 13th International Conference Interdisciplinarity in Engineering, INTER-ENG 2019, 3–4 October 2019, Targu Mures, Romania 46, 110–115.

Iskhakov, I., Ribakov, Y., Holschemacher, K., Mueller, T., 2014. Experimental Investigation of Full Scale Two-Layer Reinforced Concrete Beams. Mech. Adv. Mater. Struct. 21, 273–283.

Li, C., Zhu, H., Niu, G., Cheng, S., Gu, Z., Yang, L., 2022. Flexural behavior and a new model or flexural design of concrete beams hybridly reinforced by continuous FRP bars and discrete steel fibers. Structures 38, 949–960.